DMD Fast Forward. Published on November 25, 2015 as DOI: 10.1124/dmd.115.067868
This article has not been copyedited and formatted. The final version may differ from this version.

Pharmacokinetics and Disposition of the Thiouracil Derivative PF-06282999, an Orally Bioavailable, Irreversible Inactivator of Myeloperoxidase Enzyme, Across Animals and Humans

Jennifer Q. Dong, Manthena V. Varma, Angela Wolford, Tim Ryder, Li Di, Bo Feng, Steven G. Terra, Kazuko Sagawa, and Amit S. Kalgutkar

Pfizer Inc. Cambridge, Massachusetts (J.Q.D., A.S.K.); and Pfizer, Inc. Groton, Connecticut (M.V.V., A.W., T.R., L.D., B.F., S.G.T., K.S.)

DMD Fast Forward. Published on November 25, 2015 as DOI: 10.1124/dmd.115.067868
This article has not been copyedited and formatted. The final version may differ from this version.

Running Title: Disposition of PF-06282999 in animals and human

Address correspondence to:

Amit S. Kalgutkar, Pharmacokinetics, Dynamics, and Metabolism Department, Worldwide Research and Development, Pfizer, Inc. 610 Main St, Cambridge, MA 02139. Telephone: (617)-551-3336; E-mail: **amit.kalgutkar@pfizer.com**

Text Pages: 30

Tables: 9

Figures: 3

References: 40

Abstract: 250 words

Introduction: 617 words

Discussion: 1728 words

DMD Fast Forward. Published on November 25, 2015 as DOI: 10.1124/dmd.115.067868
This article has not been copyedited and formatted. The final version may differ from this version.

Abbreviations used are: AUC, area under plasma concentration-time curve; BEI, biliary excretion index; C_{max}, maximal plasma concentrations after oral dosing; CL_b, blood clearance; CL_p, plasma clearance; CL_{renal}, renal clearance; CL/F, apparent oral clearance; CYP, cytochrome P450; DMSO, dimethyl sulfoxide; F, oral bioavailability; GFR, glomerular filtration rate; HBSS, Hank's balanced salt solution; HEK, human embryonic kidney cells; i.v., intravenous; LC-MS/MS, liquid chromatography tandem mass spectrometry; KBF, Kidney blood flow; MDCKII-LE, low efflux Madin Darby canine kidney cells; MDR1, multidrug resistant gene 1; MPO, myeloperoxidase; NADPH, β-nicotinamide adenine dinucleotide 2′-phosphate; OAT, organic anion transporter; OCT, organic cation transporter; P_{app}, apparent permeability; PF-06282999, 2-(6-(5-chloro-2-methoxyphenyl)-4-oxo-2-thioxo-3,4-dihydropyrimidin-1(2*H*)-yl)acetamide; p.o., oral; SCHH, human hepatocytes in sandwich culture; $t_{1/2}$, half-life; T_{max}, time to reach $C_{max;}$ t_R, retention time; Vd_{ss}, apparent steady state distribution volume; V_z/F, apparent volume of distribution.

ABSTRACT

The thiouracil derivative 2-(6-(5-chloro-2-methoxyphenyl)-4-oxo-2-thioxo-3,4-dihydropyrimidin-1(2*H*)-yl)acetamide (PF-06282999) is an irreversible inactivator of myeloperoxidase, and currently in clinical trials for the potential treatment of cardiovascular diseases. Concerns over idiosyncratic toxicity arising from bioactivation of the thiouracil motif to reactive species in the liver have been largely mitigated through the physicochemical (molecular weight, lipophilicity, and topological polar surface area) characteristics of PF-06282999, which generally favor elimination via non-metabolic routes. In order to test this hypothesis, pharmacokinetics and disposition studies were initiated with PF-06282999 using animals and *in vitro* assays with the ultimate goal of predicting human pharmacokinetics and elimination mechanism(s). Consistent with its physicochemical properties, PF-06282999 was resistant to metabolic turnover from liver microsomes and hepatocytes from animals and human, and was devoid of CYP inhibition. *In vitro* transport studies suggested moderate intestinal permeability and minimal transporter-mediated hepatobiliary disposition. PF-06282999 demonstrated moderate plasma protein binding across all the species. Pharmacokinetics in preclinical species were characterized by low to moderate plasma clearances, good oral bioavailability at 3-5 mg/kg doses, and renal clearance as the projected major clearance mechanism in humans. Human pharmacokinetic predictions using single species scaling of dog and/or monkey pharmacokinetics were consistent with the parameters observed in the first-in-human study, conducted in healthy volunteers at a dose range of 20-200 mg PF-06282999. In summary, disposition characteristics of PF-06282999 were relatively similar across preclinical species and human with renal excretion of unchanged parent emerging as the principal clearance

mechanism in humans, which was anticipated based on its physicochemical properties and supported by preclinical studies.

Introduction

The hemoprotein myeloperoxidase (MPO, EC 1.11.1.7), produced in the bone marrow, is one of the major neutrophil bactericidal proteins. MPO has recently emerged as a critical modulator of inflammatory conditions including rheumatoid arthritis (Odobasic et al., 2014), chronic obstructive pulmonary disease (Churg et al., 2012), acute kidney injury (Odobasic et al., 2007), Parkinson's (Choi et al., 2005) and cardiovascular disease (Mayyas et al., 2014). High concentrations of MPO have been detected in atherosclerotic plaques (Hazell et al., 1996) and elevated MPO levels are associated with risk of cardiovascular disease in otherwise healthy individuals (Meuwese et al., 2007). Studies in MPO knockout mice have demonstrated protection from cardiac remodeling and impaired left ventricular function following surgically induced myocardial infarction (Penn, 2008).

The identification of MPO as a central player in inflammation renders this enzyme as a potential target for therapeutic interventions. Recently, our laboratory described the design, synthesis, and preclinical characterization of some novel *N*1-substituted-6-aryl-2-thiouracil analogs as mechanism-based inactivators of MPO, which culminated in the discovery of the clinical candidate 2-(6-(5-chloro-2-methoxyphenyl)-4-oxo-2-thioxo-3,4-dihydropyrimidin-1(2*H*)-yl)acetamide (PF-06282999) (Fig. 1) (Ruggeri RB, 2015). PF-06282999 is a suicide substrate of MPO with a high degree of selectivity relative to other peroxidases such as thyroid peroxidase. The inhibitory mechanism likely involves oxidation of the thiouracil sulfur atom in PF-06282999 by the compound I intermediate of oxidized MPO to yield a thiyl radical, which covalently attaches to the heme moiety, causing enzyme inactivation (Ruggeri RB, 2015). The mode of inhibition is similar to the one described with the recently reported 2-thioxanthine class of MPO inactivators (e.g., compound TX5 in Figure 1) (Tiden et al., 2011; Geoghegan et al., 2012).

From a drug design perspective, thiouracils and related analogs (e.g., thioureas and thioamides) are structural alerts, which can be metabolically activated by MPO, cytochrome P450 (CYPs), and flavin monooxygenases to electrophilic sulfenic acid and sulfonate intermediates, which are capable of covalently modifying proteins and eliciting a toxicological outcome (Hanzlik and Cashman, 1983; Henderson et al., 2004). For instance, immune-mediated hepatotoxicity and agranulocytosis associated with the clinical use of the antithyroid agent propylthiouracil has been causally linked to the oxidative bioactivation of thiouracil functionality by MPO to yield protein-reactive propylthiouracil-2-sulfenic acid and propylthiouracil-2-sulfonate metabolites, which induce the formation of the anti-neutrophil antibodies in patients with propylthiouracil-induced agranulocytosis (Lee et al., 1988; Waldhauser and Uetrecht, 1991). The risk of wayward electrophilic species arising from MPO-catalyzed oxidation of PF-06282999 was principally mitigated on the basis of its low partition ratio (~ 7.0) for MPO inactivation, which is in contrast to the very high partition ratio of 75 obtained with propylthiouracil (Ruggeri RB, 2015). Correspondingly, no glutathione conjugates of PF-06282999 were detected in incubations with recombinant human MPO/hydrogen peroxide incubations (Ruggeri RB, 2015). Likewise, reductions in lipophilicity and molecular weight in the thiouracil class of MPO inhibitors ensured that the compounds were latent towards oxidative metabolism (including bioactivation) in the liver (Ruggeri RB, 2015).

A thorough understanding of major clearance pathways and accurate prediction of human pharmacokinetics of drug candidates is a critical endeavour in drug discovery, given the intrinsic links with clinical pharmacology and/or safety, which continue to dominate attrition rates in drug development (Kola and Landis, 2004; Hay et al., 2014). Consequently, in preparation for preclinical toxicological and first-in-human clinical studies for assessment of safety, tolerability,

and pharmacokinetics, the disposition of PF-06282999 was examined in animals and *in vitro* human models. The present work summarizes the preclinical absorption, distribution, metabolism, and excretion profile of PF-06282999. Results from the preclinical studies were used to predict human pharmacokinetics including the identification of anticipated clearance pathways. The collective findings are discussed against the back drop of the single dose pharmacokinetics and major elimination mechanism of PF-06282999 in healthy human volunteers after p.o. administration.

DMD Fast Forward. Published on November 25, 2015 as DOI: 10.1124/dmd.115.067868
This article has not been copyedited and formatted. The final version may differ from this version.

Materials and Methods

Chemicals and Materials. PF-06282999 (chemical purity > 99% by HPLC and NMR) and internal standard [(2*E*)-3-(4-{[(2*S*,3*S*,4*S*,5*R*)-5-{(1*E*)-*N*-[(3-chloro-2,6-difluorobenzyl)oxy]ethanimidoyl}-3,4-dihydroxytetrahydrofuran-2-yl]oxy}-3-hydroxyphenyl)-2-methyl-*N*-[(3a*S*,4*R*,5*R*,6*S*,7*R*, 7a*R*)-4,6,7-trihydroxyhexahydro-1,3-benzodioxol-5-yl]prop-2-enamide (CP-628374) were synthesized at Pfizer Worldwide Research and Development (Groton, CT). Commercially obtained chemicals and solvents were of high-performance liquid chromatography (HPLC) or analytical grade.

Plasma Protein Binding. The extent of binding of PF-06282999 to rat (5 males/5 females), mouse (30 males/30 females), dog (5 males/5 females), monkey (5 males/5 females), and human (at least 3 males and 3 females) plasma proteins was determined using disposable rapid equilibrium dialysis (RED) device with pre-packed inserts (ThermoScientific, West Palm Beach, FL). Plasma samples were prepared by mixing PF-06282999 with plasma to produce a final incubation concentration of 2 μM for PF-06282999. Aliquots (220 μl; $n = 4$) of spiked plasma were added to the donor wells, followed by the addition of phosphate buffered saline (PBS) (350 μl; $n = 4$) to the receiver wells. The device was covered with a gas permeable membrane and agitated on an orbital shaker at approximately 450 rpm within a humidified 75% relative humidity 5% CO_2 incubator operating at 37 °C for 4.0 h. Control plasma samples (t = 0; 15 μl; $n = 2$) were prepared from the remaining spiked plasma solution. Each sample was matrix matched with buffer (45 μl) and plasma (15 μl). The samples were precipitated with a 120 μl acetonitrile solution containing 100 ng/ml of CP-628374 as internal standard. All samples for analysis were prepared in a 96-well plate, centrifuged (1900 x *g*, 5 min, room temperature), and the supernatants were transferred and analyzed by liquid chromatography tandem mass

DMD Fast Forward. Published on November 25, 2015 as DOI: 10.1124/dmd.115.067868
This article has not been copyedited and formatted. The final version may differ from this version.

spectrometry (LC-MS/MS). The fraction unbound of PF-06282999 to plasma proteins was calculated as ratio of concentration of analyte in buffer over concentration of analyte in plasma.

Blood Cell Partitioning. Blood to plasma partitioning of PF-06282999 was determined in fresh rat, mouse, dog, monkey, and human whole blood and plasma to which was added PF-06282999 to yield a final concentration of 1 μM (n = 3). Samples were incubated on an orbital shaker in a humidified CO_2 incubator for 60 min at 37°C. Post incubation, whole blood samples were either centrifuged to obtain plasma or matrix matched with appropriate blank plasma. Aliquots (20 μl) of plasma sample incubations and either plasma isolated from whole blood or matrix matched whole blood were mixed with acetonitrile (200 μl) containing CP-628374 (100 ng/ml, internal standard) and centrifuged. Supernatants were analyzed using LC-MS/MS. A blood/plasma partitioning ratio for PF-06282999 was calculated from the concentrations in blood and plasma.

***In vitro* Permeability Studies.** Apparent permeability (P_{app}) of PF-06282999 was examined in Caco-2 and low efflux Madin-Darby canine kidney (MDCKII-LE) cell lines in triplicate using previously published protocols (Frederick et al., 2009; Di et al., 2011; Varma et al., 2011). MDCKII-LE cells were established in-house and the cell-culture and experimental procedures were discussed in detail previously (Di et al., 2011). Caco-2 cells, obtained from the American Type Culture Collection (ATCC, Manassas, Manassas, VA), were seeded in 24-well Falcon Multiwell plates (polyethylene terephthalate membranes, pore size 1.0 μm) at 4.0×10^4 cells/well. Caco-2 absorptive permeability was assessed at apical/basal pH of 6.0/7.4 and 7.4/7.4. The effect of calcium-free medium and efflux inhibitor cocktail, cyclosporin A (7 μM) and verapamil (40 μM), on absorptive permeability (pH 7.4/7.4) of PF-06282999 (1 μM) was also evaluated. Permeability of nadolol, a low permeability marker, was measured to assess the cell monolayer integrity.

DMD Fast Forward. Published on November 25, 2015 as DOI: 10.1124/dmd.115.067868
This article has not been copyedited and formatted. The final version may differ from this version.

Human MDCKII-MDR1 Efflux Assay. MDCKII-multidrug resistant gene 1 (MDR1) cells were obtained from Professor Piet Borst, Netherland Cancer Institute, Amsterdam, Netherlands. The cells were seeded at a cell density of 2.5 x 10^5 cells/ml in complete MEM-α medium on Falcon/BD 96-well membrane inserts, and incubated (37 °C, 95% humidity, 5% CO_2) for 5 days. A transwell assay analogous to the one previously described (Feng et al., 2008a) was used. For apical-to-basolateral (A-to-B) permeability ($P_{app,AB}$), medium was removed from the insert on day 5. 75 µl of fresh hank's balanced salt solution (HBSS) with added components (Life Technologies, Grand Island, NY) containing PF-06282999 (2 µM) was added on the apical side and 250 µl of fresh buffer was added on the basolateral side. The plate was then incubated at 37 °C for 2 h. For B-to-A permeability ($P_{app,BA}$), medium from the insert was replaced with 75 µl of fresh buffer, and 250 µl of fresh buffer containing PF-06282999 (2 µM) was added on the basolateral side followed by incubation for 2 h at 37 °C. All studies with PF-06282999 were conducted in triplicate.

The following equations were used to calculate P_{app} values and MDR1 efflux ratio.

$$P_{app} = \frac{1}{area \bullet C_D(0)} \bullet \frac{dM_r}{dt} \qquad \textit{(Eq. 1)}$$

$$\text{Efflux ratio} = \frac{P_{app,BA}}{P_{app,AB}} \qquad \textit{(Eq. 2)}$$

Where, area is the surface area of the transwell insert, $C_D(0)$ is the initial concentration of compound applied to the donor chamber, t is incubation time, M_r is the mass of the compound in the receiver compartment, and dM_r/dt is the flux of the compound across the cell monolayer.

Liver Microsomal Stability. Pooled male Wistar-Han rat, male CD-1 mouse, male beagle dog, male cynomolgus monkey, and male and female human liver microsomes (pool of 50 livers)

DMD Fast Forward. Published on November 25, 2015 as DOI: 10.1124/dmd.115.067868
This article has not been copyedited and formatted. The final version may differ from this version.

were purchased from BD Gentest (Woburn, MA). Half-life ($t_{1/2}$) assessments in liver microsomes was determined in duplicate after incubation of PF-06282999 (1 μM) with liver microsomes (CYP concentration = 0.25 μM) in 0.1 M potassium phosphate buffer (pH 7.4) containing 1 mM $MgCl_2$ at 37 °C. The reaction mixture was prewarmed at 37 °C for 2 min before adding NADPH (1.3 mM). Aliquots of the reaction mixture at 0, 5.0, 10, 15, 30, 45 and 60 min were added to acetonitrile containing an internal standard CP-628374 (100 ng/ml), and the samples were centrifuged prior to LC-MS/MS analysis of substrate disappearance. For control experiments, NADPH and/or liver microsomes were omitted from these incubations. For the purposes of metabolite identification studies, the concentration of PF-06282999 in the microsomal incubations was raised to 10 μM and the microsomal protein concentration increased to 1.0 mg/ml. The duration of the incubation time was 45 min. Separate incubations of PF-06282999 (10 μM) were also conducted in human liver microsomes containing NADPH (1.3 mM) and glutathione (1 mM) for the purposes of trapping reactive species arising from the oxidative metabolism of PF-06282999.

Stability in Cryopreserved Hepatocytes. Cryopreserved Wistar-Han rat (male, pool of 12 donors), CD-1 mouse (male, pool of 12 donors), beagle dog (male, pool of five donors), cynomolgus monkey (male, pool of five donors), and human (pool of 10 donors of mixed gender) hepatocytes were purchased from Celsis (Chicago, IL). Williams E media was prepared by adding 26 mM sodium bicarbonate and 50 mM HEPES, followed by 0.2 μm filtration then 30 min of CO_2/O_2 bubbling at 37 °C. This medium was used for thawing suspension of hepatocytes. Incubations were conducted in a 96-well flat-bottom polystyrene plate in duplicate. Hepatocytes were suspended at 0.5 x 10^6 viable cells/ml of Williams E media and prewarmed at 37 °C for 30 min. Incubations were initiated with the addition of PF-06282999 (final

DMD Fast Forward. Published on November 25, 2015 as DOI: 10.1124/dmd.115.067868
This article has not been copyedited and formatted. The final version may differ from this version.

concentration = 1.0 μM) and were conducted at 37 °C, 75% relative humidity, and 5% CO_2. The reaction was stopped at 0, 3, 15, 30, 60, 90, or 120 min by the addition of acetonitrile (135 μl) containing an internal standard. The samples were centrifuged at ~1900 × *g* for 10 min before LC-MS/MS analysis for the disappearance of PF-06282999. For the purposes of qualitative metabolite identification studies, the concentration of PF-06282999 in the hepatocyte incubations was increased to 10 μM.

For examination of PF-06282999 depletion in cryopreserved human hepatocytes via the relay method (Di et al., 2013), the hepatocyte plate was incubated at 37 °C with 95% O_2/ 5% CO_2, 75% relative humidity for 4 h daily for 5 days. Aliquots (25 μl) of the total suspension were sampled at 0, 4, 8, 12, 16 and 20 hours and the rest of the hepatocyte incubation plate was centrifuged (~1900 x *g* , 10 min, room temperature) at the end of each relay. Aliquots (50 μl) of supernatant were sampled for quantification of concentration and 300 μl supernatant was transferred to a clean 24-well plate and stored at -80 °C until the next relay experiment. For the second relay experiment, the supernatant plate was warmed to 37 °C for 30 min and hepatocytes were added to the samples to give a final cell density 0.5 x 10^6 cells/ml. The plates were incubated at 37 °C for 4 h, sampled and processed as described above. All the samples were quenched with 2x volume of acetonitrile containing an internal standard, centrifuged and transferred for LC-MS/MS analysis. Five relays were performed to give a total incubation time of 20 h, and $t_{1/2}$ was calculated as described in the microsomal stability section. The following equations were used to calculate apparent intrinsic clearance ($CL_{int,app}$), scaled intrinsic clearance ($CL_{int,scaled}$) and hepatic blood clearance (CL_b) (Di et al., 2012).

$$\text{Hepatocyte } CL_{int,app} = \ln 2 \bullet \frac{1}{t_{1/2}\,(\text{min})} \bullet \frac{\text{mL incubation}}{0.5\,\text{M cells}} \bullet \frac{1000\,\mu\text{l}}{\text{ml}} = \mu\text{l/min/million cells}$$

DMD Fast Forward. Published on November 25, 2015 as DOI: 10.1124/dmd.115.067868
This article has not been copyedited and formatted. The final version may differ from this version.

$$\text{Hepatocyte } CL_{int,scaled} = \ln 2 \bullet \frac{1}{t_{1/2}\,(\text{min})} \bullet \frac{\text{ml incubation}}{0.5\,\text{million cells}} \bullet \frac{\text{million cells}}{\text{g liver}} \bullet \frac{\text{g liver}}{\text{kg}}$$

$$\text{Well Stirred Model } CL_b = \frac{Q \bullet (f_{up}/R_b) \bullet CL_{u,int}}{Q + (f_{up}/R_b / f_{umic}) \bullet CL_{u,int}}$$

Transport Studies using Sandwich Culture Human Hepatocytes (SCHH). Cryopreserved human hepatocytes lot Hu4241 was obtained from Life Technologies (Grand Island, NY,). The SCHH methodology applied here was described previously (Bi et al., 2006). Briefly, cryopreserved hepatocytes were thawed and plated with cell density of 0.75×10^6 cells/ml. The plates were overlaid with 0.25 mg/ml matrigel on the second day and the cultures were maintained. On day 5, the hepatocytes were preincubated for 10 min with Ca^{2+} HBSS buffer in the absence or presence of rifamycin SV (100 μM) for determination of apparent intrinsic uptake clearance ($CL_{uptake,int,app}$). For determination of apparent intrinsic biliary clearance ($CL_{biliary,int,app}$), the cells were preincubated with or without Ca^{2+} HBSS buffer for 10 min. After aspiration of the preincubation buffer, the reactions were initiated by addition of PF-06282999 (1 μM) and were terminated at predetermined time points (0.5, 1, 2, 5, 10, and 15 min) by washing the cells three times with ice-cold HBSS. Cells were then lysed with 100% methanol containing terfenadine as internal standard and the samples were analyzed by LC-MS/MS. Calculation of $CL_{uptake,int,app}$, $CL_{passive}$ (passive diffusion), $CL_{biliary,int,app}$, and biliary excretion index (BEI) were described in detail previously (Kalgutkar et al., 2007).

CYP Inhibition Studies. Reversible inhibition of major human CYP isoforms (CYP1A2, CYP2B6, CYP2C8, CYP2C9, CYP2C19, CYP2D6, and CYP3A4/5) by PF-06282999 was evaluated via incubation of standard marker substrates (phenacetin (CYP1A2), bupropion (CYP2B6), paclitaxel (CYP2C8), diclofenac (CYP2C9), *S*-mephenytoin (CYP2C19), dextromethorphan (CYP2D6), testosterone (CYP3A4/5), midazolam (CYP3A4/5), and

DMD Fast Forward. Published on November 25, 2015 as DOI: 10.1124/dmd.115.067868
This article has not been copyedited and formatted. The final version may differ from this version.

nifedipine (CYP3A4/5)) of human CYP isozymes with pooled human liver microsomes in the presence of an NADPH-regenerating system (NADP (1 mM), glucose-6-phosphate (5 mM), glucose-6-phosphate dehydrogenase (1 unit/ml)) in 50 mM potassium phosphate buffer, pH 7.4, containing 3.3 mM $MgCl_2$ and 1 mM EDTA at 37 °C open to air. The incubation volume was 0.2 ml. Microsomal protein concentrations, substrate concentrations, incubation times, and reaction termination solvents for each activity have been described in detail previously (Walsky and Obach, 2004). Incubation mixtures contained PF-06282999 at concentrations ranging from 0.1–100 μM. Stock solutions of PF-06282999 were prepared in methanol. The final concentration of methanol in the incubation mixtures was 1% (v/v).

To examine the ability of PF-06282999 to act as a time- and/or NADPH-dependent inhibitor of major human CYP isoforms, PF-06282999 (0–100 μM) was preincubated at 37 °C, in duplicate, with human liver microsomes (protein concentration 50–100 μg/ml, depending on which isozyme was assessed) in 50 mM potassium phosphate buffer, pH 7.4, containing 3.3 $MgCl_2$ and 1 mM EDTA at 37 °C in the presence and absence of an NADPH-regenerating system for approximately 30 min. After preincubation, a portion of the incubation mixture (20 μl) was added to a mixture containing a probe CYP isozyme substrate (concentration of approximately the K_m value) (Walsky and Obach, 2004) in 50 mM potassium phosphate buffer, pH 7.4, containing 3.3 mM $MgCl_2$, 1 mM EDTA, and the NADPH-regenerating system at 37°C. At the end of the incubation period (30 min), acetonitrile containing an internal standard was added, and the mixtures were centrifuged (920 x *g*, 10 min, 10°C). The supernatants were analyzed by LC-MS/MS for metabolites of probe CYP substrates using validated bioanalytical conditions established previously (Walsky and Obach, 2004). IC_{50} values for inhibition of CYP isozymes

were estimated using Galileo version 3.3 software (ThermoFisher Scientific Inc., Philadelphia, PA).

Human Renal Transporters Substrate Studies. Human embryonic kidney (HEK) 293 cells transfected with the human renal transporter proteins organic cation transporter 2 (hOCT2), organic anion transporter 1 (hOAT1), or organic anion transporter 3 (hOAT3) were generated at Pfizer (Groton, CT). Wild-type HEK293 cells were cultured in Dulbecco's modified Eagle's medium supplemented with 10% heat-inactivated fetal bovine serum. HEK-hOAT1, HEK-hOAT3, and HEK-hOCT2 cells were cultured using growth media containing hygromycin B (60 μg/ml). Cells were maintained at 37°C, 5% CO_2, and 95% relative humidity. Uptake studies utilized our previously published protocol (Feng et al., 2008b). Briefly, cells were seeded at a density of 1.12 x 10^5 cells/well in 24-well poly-D-lysine coated plates, and cultured for 48 h. Uptake buffer was prepared using HBSS, supplemented with 20 mM HEPES, at pH 7.4. Uptake was initiated by the addition of 0.1 ml uptake buffer containing varying concentrations (0.137 to 300 μM) of PF-06282999. The plates were then incubated for 4 min at 37 °C with shaking at 150 rpm. The experiment was stopped by washing the cells four times with 0.2 ml ice-cold uptake buffer/well, and then lysed with 0.2 ml of internal standard solution in 100% methanol. The lysates were analyzed by LC-MS/MS for PF-06282999.

Animal Pharmacokinetics. All experiments involving animals were conducted in our AAALAC-accredited facilities and were reviewed and approved by Pfizer Institutional Animal Care and Use Committee. Male CD-1 mice (25-35 g), Jugular vein/carotid artery double cannulated Wistar-Han rats (~250 g), obtained from Charles River Laboratories (Wilmington, MA), male Beagle dogs (~12 kg), and male cynomolgus monkeys (~7 kg) were used for these studies. Animals were fasted overnight and through the duration of the study (1.0 or 2.0 h),

whereas access to water was provided ad libitum. PF-06282999 was administered intravenously (i.v.) in either 12% sulfobutylether-β-cyclodextrin with or without 1% DMSO or 30% hydroxypropyl-β-cyclodextrin containing 5% DMSO via the tail vein (mice, *n*=3), carotid artery (rats, *n*=3), saphenous vein (dogs, *n*=3), femoral vein (monkeys, *n*=2) at a dose of 1.0 mg/kg in a dosing volume of 5 ml/kg (mice), 2 ml/kg (rats), 0.5 ml/kg (dogs), and 1 ml/kg (monkeys). Serial blood samples were collected before dosing and 0.083, 0.25, 0.5, 1, 2, 4, 7, and 24 h after dosing. PF-06282999 was also administered by p.o. gavage to mice (5 mg/kg at 5 ml/kg in 0.5% methylcellulose), rats (5 mg/kg at 2.5 ml/kg in 0.5% methylcellulose), dogs (3 mg/kg at 3 ml/kg in 0.5% methyl cellulose), and monkeys (3 mg/kg at 5 ml/kg in 5% HPMC in 20 mM Tris/0.5% HPMCA). Blood samples were taken prior to p.o. administration then serial samples were collected at 0.25, 0.5, 1, 2, 4, 7, and 24 h after dosing. Blood samples from the various pharmacokinetic studies were centrifuged to generate plasma. All plasma samples were kept frozen until analysis. Urine samples (0–7.0 and 7.0–24 h; pooled 0-24 h for mice) were also collected after i.v. administration to mice, rats, dogs, and monkeys. For mouse samples, aliquots of plasma (10 µl) or urine (2 µl mixed with 8 µl plasma) were extracted using liquid/liquid extraction with methyl-t-butyl ether containing an internal standard. For rat, dog, or monkey samples, aliquots of plasma or urine (20-25 µl) were transferred to 96-well blocks and acetonitrile (150-200 µl) containing an internal standard was added to each well. Supernatant was dried under nitrogen and reconstituted with 100 µl acetonitrile/water (1:1 with 0.1% formic acid for mice; 20:80 for dog) or added to 100 µl water without evaporation. Following extraction, the samples were then analyzed by LC-MS/MS and concentrations of analyte in plasma and urine were determined by interpolation from a standard curve.

Pharmacokinetics Studies in Humans. The phase I first-in-human study was an investigator and subject blinded (sponsor open), randomized, placebo-controlled crossover study of ascending single p.o. doses of PF-06282999 administered sequentially, at least 1 week apart, in healthy adult subjects. The study protocol and informed consent documents were approved by the institutional review board. All subjects signed an approved written informed consent form before any study-related activities for this clinical study. All subjects were male and majority of them were White (7/8, 87.5%), and of Hispanic or Latino descent. The age ranged from 22 to 46 years. The weight ranged from 70.5 to 98.2 kg, and the BMI ranged from 23.0 to 30.3 kg/m^2 across the treatment groups. No dose-limiting tolerability was noted over the dose range of 20 to 200 mg. PF-06282999 was administered as a solution [1% (w/v) methylcellulose, 0.5% (w/v) hydroxypropyl methylcellulose acetate succinate-HF, 80 mM tromethamine with a small amount of sodium hydroxide] to one cohort of 8 fasted male subjects at doses of 20, 50, 125 and 200 mg in a 4-period 4-sequence cross-over treatment design with placebo substitution (Table 1). Within each treatment period, 6 subjects were randomized to active study drug and 2 to a matching placebo. A standardized meal was provided 4 h after dosing. Blood samples were collected at intervals for up to 48 h post dose for quantitation of circulating levels of PF-06282999. Two urine samples were collected from 0 to 24 h pre- and post-dose, the volume was measured, and aliquots were examined quantitatively for PF-06282999.

Determination of Pharmacokinetic Parameters. Pharmacokinetic parameters in animals and humans were determined using noncompartmental analysis (Watson v.7.4, Thermo Scientific, Waltham, MA for animal data and a Pfizer internally validated system of non-compartmental analysis for human data). Maximum plasma concentrations (C_{max}) of PF-06282999 in plasma after p.o. dosing in preclinical species and human were determined directly from the

DMD Fast Forward. Published on November 25, 2015 as DOI: 10.1124/dmd.115.067868
This article has not been copyedited and formatted. The final version may differ from this version.

experimental data, with T_{max} defined as the time of first occurrence of C_{max}. The area under the plasma concentration-time curve from t = 0 to 24 h (AUC_{0-24}) and t = 0 to infinity ($AUC_{0-\infty}$) was estimated using the linear trapezoidal rule. In animals, systemic plasma clearance (CL_p) was calculated as the intravenous dose divided by $AUC_{0-\infty}^{i.v.}$. In humans, apparent p.o. clearance (CL/F) was calculated as the p.o. dose divided by $AUC_{0-\infty}^{p.o.}$. The terminal rate constant (k_{el}) was calculated by a linear regression of the log-linear concentration-time curve, and the terminal elimination $t_{1/2}$ was calculated as 0.693 divided by k_{el}. Apparent steady state distribution volume (Vd_{ss}) in animals and apparent volume of distribution (V_z/F) in humans were determined as the i.v. or p.o. dose divided by the product of $AUC_{0-\infty}$ and k_{el}. The absolute bioavailability (F) of the p.o. doses in animals was calculated by using the following equation: $F = AUC_{0-\infty}^{p.o.}/AUC_{0-\infty}^{i.v.} \times dose^{i.v.}/dose^{p.o.}$. Percentage of unchanged PF-06282999 excreted in urine over 24 h ($A_{e,urine,(0-24h)}$) was calculated using the following equation: amount (in mg) of PF-06282999 in urine over the 24 h interval post dose/actual amount of PF-06282999 dose administered (mg) x 100%. The renal clearance (CL_{renal}) was derived as the ratio of amount (in mg) of PF-06282999 in urine over the 24 h interval post dose/AUC_{0-24}.

LC-MS/MS Analysis for Quantitation of PF-06282999. Concentrations of PF-06282999 were determined on an AB Sciex model API-4000 LC-MS/MS triple quadrupole mass spectrometer (AB Sciex, Framingham, MA). Analytes were chromatographically separated using an Eksigent Express HT (Eksigent Technologies, Dublin, CA) or Shimadzu LC-20AD (Shimadzu Scientific Instruments, MD) pumps. An CTC PAL autosampler was programmed to inject 20 µl on a Luna C8 (3 µ) 30 x 2 mm for rat; kinetex C18 (2.6 µ) 30 x 3 mm for mouse using a mobile phase consisting of 10 mM ammonium formate buffer containing 0.1% (v/v) formic acid (solvent A) and acetonitrile (solvent B) at a flow rate of 0.5 ml/min. Ionization was conducted in the

positive ion mode at the ionspray interface temperature of 400 °C, using nitrogen for nebulizing and heating gas. The ion spray voltage was 5.0 kV and the declustering potential was optimized at 41 eV. PF-06282999 was detected using electrospray ionization in the multiple reaction monitoring mode monitoring for mass-to-charge (*m/z*) transition 326→ 155. PF-06282999 standards were fit by least-squares regression of their areas to a weighted linear equation, from which the unknown concentrations were calculated. The dynamic range of the assay was 1.0-2000 ng/ml. Assay performance was monitored by the inclusion of quality control samples with acceptance criteria of ± 30% target values.

Bioanalytical Methodology for Metabolite Identification. Qualitative assessment of the metabolism of PF-06282999 in liver microsomes and hepatocytes was conducted using a Thermo Finnegan Surveyor photodiode array plus detector, Thermo Acela pump and a Thermo Acela Autosampler (Thermoscientific, West Palm Beach, FL). Chromatography was performed on a Phenomenex Hydro RP C18 (4.6 mm x 150 mm, 3.5 µm) column (Phenomenex, Torrance, CA). The mobile phase composed of 5 mM ammonium formate buffer with 0.1% formic acid (pH=3) (solvent A) and acetonitrile (solvent B) at a flow rate of 1 ml/min. The binary gradient was as follows: solvent A to solvent B ratio was held at 95:5 (v/v) for 3 min and then adjusted to 55:45 (v/v) from 0 to 35 min, 30:70 (v/v) from 35 to 45 min, and 5:95 (v/v) from 45 to 52 min where it was held for 3 min and then returned to 95:5 (v/v) for 6 min before next analytical run. Identification of the metabolites was performed on a Thermo Orbitrap mass spectrometer operating in positive ion electrospray mode. The spray potential was 4 V and heated capillary was at 275 °C. Xcalibur software version 2.0 was used to control the HPLC-MS system. Product ion spectra were acquired at a normalized collision energy of 65 eV with an isolation width of 2 amu. Metabolites from liver microsomes or hepatocyte incubations were identified in

DMD Fast Forward. Published on November 25, 2015 as DOI: 10.1124/dmd.115.067868
This article has not been copyedited and formatted. The final version may differ from this version.

the full-scan mode (from *m/z* 100 to 850) by comparing $t = 0$ samples with $t = 45$ min (liver microsomes) 240 min (hepatocyte) samples or through comparison with synthetic standard(s), and structural information was generated from the collision-induced dissociation spectra of the protonated molecular ions (MH^+).

Pharmacokinetics Projections to Human. The single-species allometric method was used to predict human pharmacokinetic parameters of PF-06282999 (Frederick et al., 2009). CL_p and Vd_{ss} observed in preclinical species were corrected for species differences in plasma protein binding and then scaled to humans (Frederick et al., 2009). This approach uses a fixed allometric exponent of 0.75 and 1.0 for clearance and volume, respectively. Renal clearance in humans was predicted from rat, dog and monkey using the direct correlation methodology reported previously (Paine et al., 2011). Rat, dog, or monkey CL_{renal} values corrected for plasma protein binding and kidney blood flow (KBF) differences were used to predict human CL_{renal} using the following equation.

$$CL_{renal,human} = CL_{renal,animals} \bullet \left(\frac{f_{u,human}}{f_{u,animal}} \right) \bullet \left(\frac{KBF_{human}}{KBF_{animal}} \right)$$

Where f_u is fraction unbound in plasma, and KBF is kidney blood flow. Values used for rat, dog, monkey and human KBF were 52 (Hsu et al., 1975), 22 (Keil et al., 1989), 28 (Davies and Morris, 1993), and 16 ml/min/kg (Wolf et al., 1993), respectively.

DMD Fast Forward. Published on November 25, 2015 as DOI: 10.1124/dmd.115.067868
This article has not been copyedited and formatted. The final version may differ from this version.

Results

Plasma Protein Binding and Blood Cell Partitioning of PF-06282999. *In vitro* plasma protein binding of PF-06282999 was evaluated by equilibrium dialysis in rat, mouse, dog, monkey, and human plasma. The mean fraction unbound in mouse rat, dog, monkey, and human plasma was 0.451, 0.447, 0.460, 0.536, and 0.376, respectively, indicating that PF-06282999 is moderately bound to plasma proteins across preclinical species and human. PF-06282999 was stable in mouse, rat, dog, monkey, and human plasma for more than 4.0 h at 37 °C at the concentrations used in the plasma free fraction determination. The blood/plasma ratios for PF-06282999 were 1.1, 1.1, 0.91, 1.2, and 0.94 in mouse, rat, dog, monkey, and human, respectively, suggesting that PF-06282999 was equally distributed into plasma and red blood cells.

Metabolic Stability Studies with PF-06282999. PF-06282999 (1 μM) did not show metabolic turnover in NADPH-supplemented liver microsomes ($t_{1/2}$ > 120 min) and cryopreserved hepatocytes ($t_{1/2}$ > 240 min) from rat, mouse, dog, monkey, and human in the time course of incubation (60 min for liver microsomes and 120 min for hepatocytes). Furthermore, no metabolic turnover was noted in PF-06282999 (1 μM) incubations in the cryopreserved human hepatocyte assay under relay conditions ($t_{1/2}$ > 2400 min; $CL_{int,scaled}$ < 1.46 ml/min/kg, hepatic blood clearance < 0.57 ml/min/kg) (Di et al., 2013). Consistent with these findings, qualitative examination of metabolites in liver microsomes and hepatocytes from rat, mouse, dog, monkey, and human by HPLC-UV (λ = 254 nm) revealed only trace levels of three metabolites, designated as M1, M2, and M3 (Table 2). In liver microsomes, the three metabolites were formed in a NADPH-dependent fashion, suggestive of a role for CYP or flavin monooxygenase enzymes in the oxidative metabolism of PF-06282999.

DMD Fast Forward. Published on November 25, 2015 as DOI: 10.1124/dmd.115.067868
This article has not been copyedited and formatted. The final version may differ from this version.

PF-06282999 had a retention time (t_R) of ~ 29.0 min on HPLC and showed an exact mass of *m/z* 326.0361 (MH^+). Its MS^2 product ion spectrum showed diagnostic fragment ions at *m/z* 281.0144, 222.0315, and 155.0256, respectively. The ions at *m/z* 281 and 222 resulted from neutral losses of formamide and isothiocyanic acid, respectively, whereas the ion at *m/z* 155 resulted from the formation of a tropylium ion from the chloromethoxybenzene moiety.

Metabolite M1 had a t_R of ~21.9 min on HPLC and an exact mass of *m/z* 296.0433, which was 30 Da less than that of PF-06282999. The mass spectrum contained fragment ions at *m/z* 251.0214, 235.0265, and 208.0156. The ion at *m/z* 208, which was 14 Da less than the parent product ion at *m/z* 222, suggested a loss of a methyl group from the aromatic ether motif. The fragment ion at *m/z* 251, which was 30 Da less than the parent ion, suggested loss of a methyl group (- 14 Da), and replacement of the sulfur (- 32 Da) with an oxygen atom (+ 16 Da). This information suggested that M1 resulted from oxidative desulfurization and *O*-demethylation of the chloromethoxyphenyl moiety.

Metabolite M2 had a t_R of ~24.1 min on HPLC and an exact mass of *m/z* 312.0204, which was 14 Da less than that of PF-06282999. The mass spectrum contained fragment ions at *m/z* 266.9986 and 208.0157. The ions at *m/z* 267, and 208, which were 14 Da less then parent product ions at *m/z* 281 and 222 suggested M2 was derived from an *O*-demethylation of the methoxyphenyl group in PF-06282999.

Metabolite M3 had a t_R of ~25.7 min on HPLC and an exact mass of *m/z* 310.0589 (MH^+), which was 16 Da less than that of PF-06282999. The mass spectrum contained fragment ions at *m/z* 265.0372, 222.0314, and 155.0253. The ions at *m/z* 222 and 155 were also observed in the mass spectrum of the parent compound, indicating that the 6-aryl substituent was unaltered. The fragment ion at *m/z* 265, which was 16 Da less than the parent product ion *m/z* 281, suggested

oxidative desulfurization of the thiouracil motif. An authentic standard of the proposed metabolite 2-(6-(5-chloro-2-methoxyphenyl)-2,4-dioxo-3,4-dihydropyrimidin-1(2*H*)-yl)acetamide (PF-06428486) was found to have an identical t_R and mass spectrum (data not shown).

Due to the lack of metabolic turnover of PF-06282999 in human liver microsomes, human CYP enzyme(s) responsible for oxidative metabolism of PF-06282999 could not be identified using prototypic methodology (e.g., use of selective CYP enzyme inhibitors or recombinant CYPs). Overall, the qualitative biotransformation study suggests that the metabolic routes of PF-06282999 are similar in all species with no evidence of human specific metabolites. Finally, no glutathione conjugates were detected in human liver microsomal incubations of PF-06282999 in the presence of NADPH and excess glutathione, suggesting that no reactive species was released in the course of oxidative metabolism of PF-06282999.

Human CYP Isozyme Inhibition with PF-06282999. PF-06282999 exhibited no relevant reversible (IC_{50} > 100 μM) and time- or NADPH-dependent (IC_{50} > 100 μM) inhibitory effects against CYP1A2 (phenacetin-*O*-dealkylation), CYP2B6 (bupropion hydroxylation), CYP2C8 (paclitaxel-6α -hydroxylation), CYP2C9 (diclofenac-4'-hydroxylation), CYP2C19 (S-mephenytoin-4'-hydroxylation), CYP2D6 (dextromethorphan-*O*-demethylation), or CYP3A4/5 (testosterone-6β-hydroxylase, midazolam-1'-hydroxylase, and nifedipine oxidase) activities. IC_{50} values for reversible and time-dependent inhibition could not be calculated because PF-06282999 did not inhibit any CYP activity more than 30% at the highest concentration tested. Under the present experimental conditions, known CYP isozyme-specific inhibitors α-naphthoflavone, orphenadrine, montelukast, sulfaphenazole, modafinil, quinidine, and ketoconazole demonstrated potent competitive inhibition of CYP1A2, 2B6, 2C8, 2C9, 2C19, 2D6, and 3A4/5 activity, respectively, in human liver microsomes (Pfizer data on file).

Likewise, metabolism-dependent inhibition of CYP activity was also noted with the respective positive control compounds [furafylline (CYP1A2), phencyclidine (CYP2B6), gemfibrozil glucuronide (CYP2C8), tienilic acid (CYP2C9), (*S*)-fluoxetine (CYP2C19), paroxetine (CYP2D6), troleandomycin (CYP3A4/5)] in a time- and NADPH-dependent fashion (Pfizer data on file).

Absorptive Permeability of PF-06282999. The P_{app} value of PF-06282999 across Caco-2 cell monolayer (Table 3) in the A-to-B direction was 2.7 x 10^{-6} cm/s, which is comparable to drugs exhibiting moderate oral absorption in humans (Varma et al., 2012). Under identical experimental conditions, the secretory (B-to-A) permeability of PF-06282999 was 10 x 10^{-6} cm/s (efflux ratio = 3.8), suggesting that PF-06282999 is a substrate for efflux transport(s). As such, PF-06282999 was found to be a substrate for MDR1 based on bi-directional transport study using the MDCKII-MDR1 cell monolayer with a low efflux ratio of 3.3. This finding is consistent with the reduction in efflux ratio to 1.1 noted in the Caco-2 assay in the presence of the MDR1 inhibitors of verapamil and cyclosporin A.

$P_{app,AB}$ in Caco-2 was not affected by the apical pH with $P_{app,AB}$ at pH 6.0/7.4 and 7.4/7.4 estimated to be ~ 2.7 x 10^{-6} cm/s. In the absence of calcium in the media, the $P_{app,AB}$ value of PF-06282999 increased by 4.4-fold to 12 x 10^{-6} cm/s. The $P_{app,AB}$ values for PF-06282999 in the Caco-2 assay are consistent with its measured permeability of 2.2 x 10^{-6} cm/s in MDCKII-LE cells. Nadolol, a low permeability paracellular marker, showed absorptive permeability of about 0.9 x 10^{-6} cm/s at apical pH of both 6.0 and 7.4 in the Caco-2 studies. Overall, PF-06282999 demonstrates moderate permeability via both paracellular and transcellular pathways and is a substrate of MDR1 with a low efflux ratio.

Hepatobiliary Transport of PF-06282999 in SCHH. The hepatobiliary transport of PF-06282999 was examined in SCHH (Bi et al., 2006). Compared to rosuvastatin, PF-06282999 exhibited low total uptake clearance and biliary intrinsic clearance (Table 4). The corresponding mean BEI for rosuvastatin and PF-06282999 was 49% and 11%, respectively. Rifamycin SV, a pan inhibitor of transporters, had a small impact (~25%) on the uptake of PF-06282999; in contrast, rifamycin SV inhibited ~90% of rosuvastatin uptake. These observations suggest that the contribution of transporter-mediated hepatobiliary disposition to the overall clearance of PF-06282999 is likely minimal.

PF-06282999 Uptake by Major Human Renal Transporters. Substrate affinity to the major human renal anion (hOAT1 and hOAT3) and cation (hOCT2) transporters was evaluated using HEK 293 cells transfected with hOAT1-, hOAT3-, and hOCT2 transporters. No significant difference in PF-06282999 (0.1–900 μM) uptake by these transporters versus wild-type HEK 293 cells was observed (data not shown), indicating that PF-06282999 is not transported by the major human renal uptake transporters.

Pharmacokinetics of PF-06282999 after Single Doses to Animals. The pharmacokinetic parameters describing the disposition of PF-06282999 after i.v. and p.o. administration in preclinical species is shown in Table 5. PF-06282999 demonstrated low plasma clearance in mice (10.1 ml/min/kg), dogs (3.39 ml/min/kg), monkeys (10.3 ml/min/kg) and moderate clearance in rats (41.8 ml/min/kg). PF-06282999 was well distributed with Vd_{ss} ranging from 0.5–2.1 l/kg in mice, rats, dogs, and monkeys. The terminal elimination $t_{1/2}$ ranged from 0.75 to 3.3 h in the four species. Following p.o. administration at a single p.o. doses of 3 or 5 mg/kg, PF-06282999 was rapidly (T_{max} = 0.7–1.70 h) and well absorbed in mice, rats, dogs, and monkeys with F values of 100%, 86%, 75% and 76%, respectively.

Table 6 depicts data for renal excretion of unchanged PF-06282999 in preclinical species following i.v. administration. The unbound renal clearance ($CL_{renal,u}$) in mice and dogs was lower than the glomerular filtration rate (GFR) suggesting lack of active tubular secretion. However, in rats and monkeys, the unbound $CL_{renal,u}$ values of 28.3 ml/min/kg and 3.70 ml/min/kg exceeded the GFR of 8.7 ml/min/kg and 2.0 ml/min/kg (Lin, 1995) by ~ 3.20- and 1.86-fold, respectively, implying that PF-06282999 is subjected to active tubular secretion mediated by transporters in these species.

Prediction of Human Pharmacokinetics. PF-06282999 was resistant to metabolic turnover in human liver microsomes and hepatocytes under relay conditions, suggesting that metabolism would be inconsequential as a clearance mechanism in human. Furthermore, SCHH studies indicated that hepatobiliary disposition of unchanged PF-06282999 in humans is likely to be insignificant as an elimination mechanism. We therefore hypothesized that the PF-06282999 would be cleared predominantly as unchanged form via renal excretion in humans. The observation that all preclinical species exhibited some degree of renal excretion and the similarity in physicochemical properties of PF-06282999 with literature drugs (e.g., acetazolamide, furosemide, captopril, and methotrexate etc.) conducive to renal elimination (Varma et al., 2009) further supported this hypothesis. Consequently, human pharmacokinetics (CL_p and Vd_{ss}) (Table 7) were predicted from single species scaling of animal pharmacokinetics (corrected for plasma protein binding differences) (Frederick et al., 2009), and estimates of human CL_{renal} (Table 7) were obtained from rat, dog, or monkey CL_{renal} data normalized for plasma protein binding and KBF differences as reported previously (Paine et al., 2011). Overall, this exercise led to predicted parameters comprising of low to moderate CL_p (1.8–8.6 ml/min/kg or 126 –600 ml/min for a 70 kg adult) and Vd_{ss} (0.4–1.8 l/kg or 28–126 l for a 70 kg adult), and a

DMD Fast Forward. Published on November 25, 2015 as DOI: 10.1124/dmd.115.067868
This article has not been copyedited and formatted. The final version may differ from this version.

relatively short predicted $t_{1/2}$ of 2.4–2.7 h, derived from the equation $t_{1/2} = 0.693 \times Vd_{ss}/CL_p$. We assumed that the high oral bioavailability of PF-06282999 observed in animals ($F \geq 75\%$) would also be translated in humans especially at relatively low doses (20–200 mg) where absorption would not be negatively impacted by solubility and permeability. Considering that PF-06282999 was metabolically stable in human hepatocytes (under relay conditions), first pass metabolism was not anticipated to contribute significantly as a deterrence to oral absorption.

Clinical Pharmacokinetics of PF-06282999. A total of 8 subjects were randomized and treated at each of the 4 periods with a single p.o. dose of PF-06282999 or placebo. Mean plasma PF-06282999 concentration-time profiles across the studied doses are presented in Fig. 2. Plasma pharmacokinetic parameters from the non-compartmental analysis are summarized in Table 8. Following single p.o. doses of up to 200 mg PF-06282999 in solution, oral absorption of PF-06282999 was rapid with mean peak plasma concentrations achieved within 1 h post dose (Fig. 2A and 2B). Exposures as estimated by AUC and C_{max} after an p.o. dose were dose proportional up to 200 mg (Fig. 3A), and the overall mean plasma elimination $t_{1/2}$ was comparable at all dose levels with mean values of approximately 4.3 to 4.4 hours (Table 8). Renal excretion of PF-06282999 was dose-proportional, and appeared to be the predominant elimination pathway with approximately 75% of dose excreted as parent within 24 h post-dose at the 200 mg dose (Table 9 and Fig. 3B). The mean unbound renal clearance of >300 ml/min (renal clearance ranging 127-151 ml/min) exceeded the GFR of 106 ± 18 ml/min/1.73 m^2 reported for healthy adults (Soares et al., 2013), indicating potential active tubular secretion of PF-06282999. The $t_{1/2}$ (4.3–4.4 h) observed in the clinic was within 2.0-fold of the predicted value (2.4–2.7 h).

Discussion

PF-06282999 is a low molecular weight (326Da), hydrophilic (cLogP = 0.49, $LogD_{7.4}$ = 0.81, topological polar surface area = 84.66 $Å^2$), weak acid (pKa = 7.82) (Ruggeri RB, 2015). Consistent with its physicochemical attributes, PF-06282999 was virtually resistant towards metabolic turnover in NADPH-supplemented liver microsomes and hepatocytes from preclinical species and human, was devoid of glutathione conjugate formation in human liver microsomes and hepatocytes, and caused no reversible or time- and NADPH-dependent inhibition of major human CYP isoforms. Because trace levels of oxidative metabolites were noted in human liver microsomal and hepatocyte incubations of PF-06282999 (Table 2), we initially speculated that a proportion of the clearance mechanism of PF-06282999 in humans would be dictated by slow metabolism. Metabolic turnover rates for slowly metabolized compounds cannot be estimated in standard hepatocyte assays involving short incubation periods. Recently, a novel human hepatocyte suspension relay assay was utilized to extend drug residence time in cryopreserved hepatocytes, which provided reliable estimates of *in vitro* intrinsic clearance for slowly metabolized compounds (Di et al., 2013). Even under extended incubations, PF-06282999 was stable towards metabolic turnover, which implied that metabolic elimination would be inconsequential as an elimination mechanism in humans. Furthermore, the possibility of hepatobiliary disposition of unchanged PF-06282999 mediated by uptake and efflux transporters was explored in human hepatocytes under sandwich culture conditions (Table 4). Rifamycin SV, a pan inhibitor of transporters, had minimal impact on the hepatic uptake of PF-06282999, and the biliary excretion index, an indication of extent of biliary secretion, was found to be low. Collectively, hepatic clearance involving metabolizing enzymes and drug transporters has a minimal role in the systemic clearance of PF-06282999.

On the basis of physicochemical properties and membrane permeability, PF-06282999 fit into extended clearance classification system (ECCS) class 3A, where renal clearance is predicted to be the major clearance mechanism in human (Varma et al., 2015). Consistent with this, preclinical findings implied that PF-06282999 would be cleared unchanged via renal clearance, which was subsequently confirmed in the first-in-human study (e.g., ~75% of the dose excreted unchanged in urine at the 200 mg p.o. dose). Against this backdrop, it is noteworthy to point out that percentage of PF-06282999 dose excreted in the urine following i.v. administration in preclinical species was less than 50%, despite the lack of metabolic turnover detected in the time course of the *in vitro* assays using animal hepatic tissue (30 min incubation for liver microsomes and 120 min for hepatocytes). This may suggest additional *in vivo* clearance pathways for PF-06282999 such as slow metabolism (low turnover rates *in vitro* but a relatively higher extent of metabolism *in vivo*) (Chan et al., 2013) and/or biliary elimination in the preclinical species, especially the rat, where the systemic CL_p (41.8 ml/min/kg) is in the moderate range. Alternative clearance mechanism may be a possibility to some degree in humans as well. For example, elimination of approximately 75% of the dose in urine at the 200 mg dose suggests that the remainder (25%) of the dose could be cleared through metabolic or biliary excretion routes. However, the possibility remains that 25% of the p.o. dose is not orally absorbed. Radiolabeled mass balance/excretion route studies and absolute oral bioavailability studies with PF-06282999 should shed additional light on the similarities/differences in excretion profile between animals and humans.

The predominantly renal elimination pathway of PF-06282999 in humans is not altogether surprising. The physicochemical attributes of PF-06282999 coupled with the measured thermodynamic solubility (crystalline form) of 0.184 mg/ml in phosphate buffered saline (PBS)

at pH 6.5 and 0.166 mg/ml in unbuffered water, and moderate passive MDCKII-LE permeability (~2.2 x10^{-6} cm/s), would ultimately manifest into a solubility-limited and/or permeability-limited absorption depending on the dose and CL_{renal} as the likely clearance mechanism (Varma et al., 2009; Varma et al., 2012).

Renal transporters including hOAT1, hOAT3, and hOCT2 are major transporters expressed on the basolateral membrane involved in the active renal secretion, while MDR1, breast cancer resistant protein, multidrug resistant-associated proteins, and multidrug and toxic compound extrusion 1/2K transporters can potentially mediate secretion across the apical membrane (Masereeuw and Russel, 2001). PF-06282999 is not a substrate to hOAT1, hOAT3 and hOCT2, but is a substrate of MDR1. Consequently, the > 3.0-fold increase in human $CL_{renal,u}$ (> 300 ml/min) of PF-06282999 over the human GFR could be accounted for, by an active secretion process in the renal elimination of PF-06282999, mediated by efflux transporter MDR1 coupled with unknown renal uptake transporters. If so, then it is tempting to speculate that species differences in MDR1 expression in the kidney and/or PF-06282999 affinity towards MDR1 would partially account for the differences in $CL_{renal,u}$ exceeding GFR in rats (3.2-fold of GFR), monkeys (1.86-fold of GFR) and human (3.3-fold of GFR), but not in dogs and mice. Although quantitative information of species difference of MDR1 expression is limited, fairly good correlation was found in the MDR1 efflux activity between human and monkey, which could be due to high homology of the amino acid sequences (96% similarity) (Takeuchi et al., 2006). Also, efflux activity of human MDR1 showed a relatively better correlation with rat Mdr1a and Mdr1b compared to the correlation with mouse or canine efflux activity, although the substrate affinity was maintained across the species. Interestingly, these observations are consistent with the PF-06282999 net secretion noted in the human, rat and monkey, but not in mouse and dog.

DMD Fast Forward. Published on November 25, 2015 as DOI: 10.1124/dmd.115.067868
This article has not been copyedited and formatted. The final version may differ from this version.

Nevertheless, further understanding on the mechanisms involved in the renal secretion and the observed species difference is warranted.

While transporters can exhibit significant species differences in terms of expression level and functional activity (Chu et al., 2013), it is noteworthy to point out that human CL_{renal} of 36 structurally diverse drugs was reasonably well predicted using dog CL_{renal} after correcting for plasma protein binding and KBF (Paine et al., 2011). The clinical pharmacokinetics of PF-06282999 after p.o. administration (20–200 mg) (Table 8) were characterized by a low systemic CL/F (186–197 ml/min or 2.6–2.8 ml/min/kg for a 70 kg adult) and a moderate V_z/F (68.9–73.7 l or 0.98–1.05 l/kg for a 70 kg adult), which led to a relatively short $t_{1/2}$ (4.3–4.4 h). Normalization of CL/F values for the 20–200 mg dose range shown in Table 8 with approximate F values corresponding to the percentage of dose excreted in urine in a 24 h period at these doses (Table 9), yielded CL_p ranging from ~ 124–149 ml/min or 1.8–2.1 ml/min/kg (for a 70 kg adult), which were reasonably well predicted (± 2-fold) from the single species scaling of dog (CL_p ~ 1.8 ml/min/kg) and monkey (CL_p ~ 3.4 ml/min/kg) (see Table 7). In contrast, rat overpredicted the human CL_p by ~ 4-fold, which implies that clearance mechanisms in addition to renal elimination are operative in the rat, and will need additional investigations via metabolic stability assessments in rat hepatocytes under relay conditions and biliary excretion studies. In a similar fashion, p.o. V_z/F (68.9–73.7 l) values were normalized for F equal to the percentage of dose excreted in urine, yielding Vd_{ss} ranging from 45.9–54.8 l or 0.65–0.78 l/kg, which were predicted from single species scaling of dog (0.4 l/kg) and monkey (0.8 l/kg) Vd_{ss} (Table 7). Despite the subtle nuances in CL_p and Vd_{ss} predictions from single species scaling of animal pharmacokinetics data, it is interesting to note that all preclinical species ultimately predicted a

DMD Fast Forward. Published on November 25, 2015 as DOI: 10.1124/dmd.115.067868
This article has not been copyedited and formatted. The final version may differ from this version.

short $t_{1/2}$ (2.4–2.7 h) for PF-06282999 in humans, which is in close proximity to the observed values (3.9–4.2 h) generated from the CL_p and Vd_{ss} estimates at the various dose range.

While the human pharmacokinetics prediction utilizing the dog or monkey were fairly accurate, prediction of human $CL_{renal,}$ the predominant clearance mechanism of PF-06282999, using dog and/or monkey CL_{renal} normalized for plasma free fraction and KBF differences and the direct correlations methodology of Paine *et al*. (Paine et al., 2011) led to > 2.5–3.0-fold under-prediction (predicted human CL_{renal} = 0.6 (dog)–0.7 (monkey) ml/min/kg; observed p.o. CL_{renal} in humans = 127–151 ml/min or 1.81–2.15 ml/min/kg). In contrast, rat CL_{renal} after correction for plasma unbound fraction and KBF differences led to a predicted human CL_{renal}, value of 3.00 ml/min/kg, which was in close proximity to the observed value. Suffice to say, with the exceptions of some anionic compounds, human CL_{renal} was also reasonably well predicted from rat CL_{renal} in the work of Paine et al. (Paine et al., 2011). Additionally, $CL_{renal,u}$ exceeding GFR in rats (3.2-fold of GFR) similar to that in human (3.3-fold of GFR), but not in dogs, could explain to a better prediction of human CL_{renal} from rat, but an under prediction using dog CL_{renal}.

Based on an analysis of MDCKII-LE permeability versus human intestinal absorption for 105 marketed drugs, compounds with P_{app} of > 5 x 10^{-6} cm/s are most likely to demonstrate complete oral absorption when solubility is not a limiting factor, while a P_{app} range of 2–5 x 10^{-6} cm/s represent compounds with human intestinal absorption in the moderate range (~30–80%) (Varma et al., 2012). In alignment with the *in vitro* permeability data, oral bioavailability studies were indicative of good oral absorption (oral F > 75%) in preclinical species at relatively low dose. For the preliminary clinical pharmacokinetics studies at the 20–200 mg dose range, PF-06282999 was solubilized in Tris buffer (pH adjusted with NaOH) containing 0.5% hydroxypropyl methylcellulose acetate succinate to prevent precipitation to eliminate any

potential solubility limited absorption. PF-06282999 was rapid absorbed (T_{max} = 0.5–0.75 h) in humans when administered orally as a solution, which suggested good permeation in the upper gastrointestinal tract. Likewise, based on the renal excretion data (~ 75% of the 200 mg dose excreted unchanged in urine), it is safe to assume that the oral F of PF-06282999 is at least 75% at the 200 mg dose.

In conclusion, our present study provides key information regarding the disposition characteristics of PF-06282999, a novel mechanism-based inactivator of MPO, in preclinical species and humans. Renal clearance of unchanged PF-06282999 emerged as the principal clearance mechanism in humans, a phenomenon that was consistent with the physicochemical and permeability characteristics as defined by extended clearance classification system. Furthermore, human pharmacokinetics of PF-06282999 were reasonably well predicted from single species scaling of dog and/or monkey pharmacokinetics data, corrected for plasma free fraction differences. Selective inhibition of MPO relative to other peroxidases (e.g., thyroid peroxidases), renal elimination with minimal hepatic oxidative metabolism, and absence of mechanism-based CYP inhibition by PF-06282999 provides a strong rationale for mitigating idiosyncratic toxicity and drug-drug interaction risks with a drug candidate containing a structural alert.

Acknowledgments

The authors thank Samuel Bell, Karen Atkinson, Yi-An Bi, Renato Scialis, and Charles Rotter for assistance with the formulation support and the execution of metabolic stability and transporter studies. The authors thank Vu Le for providing statistical guidance.

DMD Fast Forward. Published on November 25, 2015 as DOI: 10.1124/dmd.115.067868
This article has not been copyedited and formatted. The final version may differ from this version.

Authorship Contributions

Participated in research design: Dong, Wolford, Kalgutkar, and Terra,

Conducted experiments: Dong, Wolford, and Ryder

Contributed new reagents or analytic tools: Di

Performed data analysis: Dong, Wolford, and Kalgutkar

Wrote or contributed to the writing of the manuscript: Dong, Varma, Di, Feng, Terra, Sagawa, and Kalgutkar

References

Bi YA, Kazolias D, and Duignan DB (2006) Use of cryopreserved human hepatocytes in sandwich culture to measure hepatobiliary transport. *Drug metabolism and disposition: the biological fate of chemicals* **34:**1658-1665.

Chan TS, Yu H, Moore A, Khetani SR, and Tweedie D (2013) Meeting the challenge of predicting hepatic clearance of compounds slowly metabolized by cytochrome P450 using a novel hepatocyte model, HepatoPac. *Drug metabolism and disposition: the biological fate of chemicals* **41:**2024-2032.

Choi DK, Pennathur S, Perier C, Tieu K, Teismann P, Wu DC, Jackson-Lewis V, Vila M, Vonsattel JP, Heinecke JW, and Przedborski S (2005) Ablation of the inflammatory enzyme myeloperoxidase mitigates features of Parkinson's disease in mice. *The Journal of neuroscience : the official journal of the Society for Neuroscience* **25:**6594-6600.

Chu X, Bleasby K, and Evers R (2013) Species differences in drug transporters and implications for translating preclinical findings to humans. *Expert opinion on drug metabolism & toxicology* **9:**237-252.

Churg A, Marshall CV, Sin DD, Bolton S, Zhou S, Thain K, Cadogan EB, Maltby J, Soars MG, Mallinder PR, and Wright JL (2012) Late intervention with a myeloperoxidase inhibitor stops progression of experimental chronic obstructive pulmonary disease. *American journal of respiratory and critical care medicine* **185:**34-43.

Davies B and Morris T (1993) Physiological parameters in laboratory animals and humans. *Pharmaceutical research* **10:**1093-1095.

Di L, Atkinson K, Orozco CC, Funk C, Zhang H, McDonald TS, Tan B, Lin J, Chang C, and Obach RS (2013) In vitro-in vivo correlation for low-clearance compounds using hepatocyte relay method. *Drug metabolism and disposition: the biological fate of chemicals* **41:**2018-2023.

Di L, Keefer C, Scott DO, Strelevitz TJ, Chang G, Bi YA, Lai Y, Duckworth J, Fenner K, Troutman MD, and Obach RS (2012) Mechanistic insights from comparing intrinsic clearance values between human liver microsomes and hepatocytes to guide drug design. *European journal of medicinal chemistry* **57:**441-448.

Di L, Whitney-Pickett C, Umland JP, Zhang H, Zhang X, Gebhard DF, Lai Y, Federico JJ, 3rd, Davidson RE, Smith R, Reyner EL, Lee C, Feng B, Rotter C, Varma MV, Kempshall S, Fenner K, El-Kattan AF, Liston TE, and Troutman MD (2011) Development of a new permeability assay using low-efflux MDCKII cells. *Journal of pharmaceutical sciences* **100:**4974-4985.

Feng B, Mills JB, Davidson RE, Mireles RJ, Janiszewski JS, Troutman MD, and de Morais SM (2008a) In vitro P-glycoprotein assays to predict the in vivo interactions of P-glycoprotein with drugs in the central nervous system. *Drug metabolism and disposition: the biological fate of chemicals* **36:**268-275.

Feng B, Obach RS, Burstein AH, Clark DJ, de Morais SM, and Faessel HM (2008b) Effect of human renal cationic transporter inhibition on the pharmacokinetics of varenicline, a new therapy for smoking cessation: an in vitro-in vivo study. *Clinical pharmacology and therapeutics* **83:**567-576.

Frederick KS, Maurer TS, Kalgutkar AS, Royer LJ, Francone OL, Winter SM, Terra SG, Chen D, and Gao X (2009) Pharmacokinetics, disposition and lipid-modulating activity of 5-{2-[4-(3,4-difluorophenoxy)-phenyl]-ethylsulfamoyl}-2-methyl-benzoic acid, a potent and subtype-selective peroxisome proliferator-activated receptor alpha agonist in preclinical species and human. *Xenobiotica; the fate of foreign compounds in biological systems* **39:**766-781.

Geoghegan KF, Varghese AH, Feng X, Bessire AJ, Conboy JJ, Ruggeri RB, Ahn K, Spath SN, Filippov SV, Conrad SJ, Carpino PA, Guimaraes CR, and Vajdos FF (2012) Deconstruction of activity-

dependent covalent modification of heme in human neutrophil myeloperoxidase by multistage mass spectrometry (MS(4)). *Biochemistry* **51:**2065-2077.

Hanzlik RP and Cashman JR (1983) Microsomal metabolism of thiobenzamide and thiobenzamide S-oxide. *Drug metabolism and disposition: the biological fate of chemicals* **11:**201-205.

Hay M, Thomas DW, Craighead JL, Economides C, and Rosenthal J (2014) Clinical development success rates for investigational drugs. *Nature biotechnology* **32:**40-51.

Hazell LJ, Arnold L, Flowers D, Waeg G, Malle E, and Stocker R (1996) Presence of hypochlorite-modified proteins in human atherosclerotic lesions. *The Journal of clinical investigation* **97:**1535-1544.

Henderson MC, Krueger SK, Stevens JF, and Williams DE (2004) Human flavin-containing monooxygenase form 2 S-oxygenation: sulfenic acid formation from thioureas and oxidation of glutathione. *Chemical research in toxicology* **17:**633-640.

Hsu CH, Kurtz TW, Preuss HG, and Weller JM (1975) Measurement of renal blood flow in the rat. *Proceedings of the Society for Experimental Biology and Medicine Society for Experimental Biology and Medicine* **149:**470-472.

Kalgutkar AS, Feng B, Nguyen HT, Frederick KS, Campbell SD, Hatch HL, Bi YA, Kazolias DC, Davidson RE, Mireles RJ, Duignan DB, Choo EF, and Zhao SX (2007) Role of transporters in the disposition of the selective phosphodiesterase-4 inhibitor (+)-2-[4-({[2-(benzo[1,3]dioxol-5-yloxy)-pyridine-3-carbonyl]-amino}-methyl)-3-fl uoro-phenoxy]-propionic acid in rat and human. *Drug metabolism and disposition: the biological fate of chemicals* **35:**2111-2118.

Keil J, Lehnfeld R, Reinhardt HW, Mohnhaupt R, and Kaczmarczyk G (1989) Acute effects of angiotensin II on renal haemodynamics and excretion in conscious dogs. *Renal physiology and biochemistry* **12:**238-249.

Kola I and Landis J (2004) Can the pharmaceutical industry reduce attrition rates? *Nature reviews Drug discovery* **3:**711-715.

Lee E, Miki Y, Hosokawa M, Sayo H, and Kariya K (1988) Oxidative metabolism of propylthiouracil by peroxidases from rat bone marrow. *Xenobiotica; the fate of foreign compounds in biological systems* **18:**1135-1142.

Lin JH (1995) Species similarities and differences in pharmacokinetics. *Drug metabolism and disposition: the biological fate of chemicals* **23:**1008-1021.

Masereeuw R and Russel FG (2001) Mechanisms and clinical implications of renal drug excretion. *Drug metabolism reviews* **33:**299-351.

Mayyas FA, Al-Jarrah MI, Ibrahim KS, and Alzoubi KH (2014) Level and significance of plasma myeloperoxidase and the neutrophil to lymphocyte ratio in patients with coronary artery disease. *Experimental and therapeutic medicine* **8:**1951-1957.

Meuwese MC, Stroes ES, Hazen SL, van Miert JN, Kuivenhoven JA, Schaub RG, Wareham NJ, Luben R, Kastelein JJ, Khaw KT, and Boekholdt SM (2007) Serum myeloperoxidase levels are associated with the future risk of coronary artery disease in apparently healthy individuals: the EPIC-Norfolk Prospective Population Study. *Journal of the American College of Cardiology* **50:**159-165.

Odobasic D, Kitching AR, Semple TJ, and Holdsworth SR (2007) Endogenous myeloperoxidase promotes neutrophil-mediated renal injury, but attenuates T cell immunity inducing crescentic glomerulonephritis. *Journal of the American Society of Nephrology : JASN* **18:**760-770.

Odobasic D, Yang Y, Muljadi RC, O'Sullivan KM, Kao W, Smith M, Morand EF, and Holdsworth SR (2014) Endogenous myeloperoxidase is a mediator of joint inflammation and damage in experimental arthritis. *Arthritis & rheumatology* **66:**907-917.

Paine SW, Menochet K, Denton R, McGinnity DF, and Riley RJ (2011) Prediction of human renal clearance from preclinical species for a diverse set of drugs that exhibit both active secretion and net reabsorption. *Drug metabolism and disposition: the biological fate of chemicals* **39:**1008-1013.

Penn MS (2008) The role of leukocyte-generated oxidants in left ventricular remodeling. *The American journal of cardiology* **101:**30D-33D.

Ruggeri RB KA, Buckbinder L, Bagley SW, Carpino PA, Conn EL, Dowling MS, Fernando DP, Jiao W, Kung DW, Orr ST, Qi Y, Rocke BN, Smith A, Warmus JS, Zhang Y, Bowles D, Widlicka DW, Eng H, Ryder T, Sharma R, Wolford A, Okerberg C, Walters K, Maurer TS, Zhang Y, Bonin PD, Spath SN, Xing G, Hepworth D, Ahn K. (2015) Discovery of 2-(6-(5-chloro-2-methoxyphenyl)-4-oxo-2-thioxo-3,4-dihydropyrimidin-1(2H)-yl)acetamide (PF-2999): A highly selective mechanism-based myeloperoxidase inhibitor for the treatment of cardiovascular diseases. *Journal of medicinal chemistry* **58:**8513-8528.

Soares AA, Prates AB, Weinert LS, Veronese FV, de Azevedo MJ, and Silveiro SP (2013) Reference values for glomerular filtration rate in healthy Brazilian adults. *BMC nephrology* **14:**54.

Takeuchi T, Yoshitomi S, Higuchi T, Ikemoto K, Niwa S, Ebihara T, Katoh M, Yokoi T, and Asahi S (2006) Establishment and characterization of the transformants stably-expressing MDR1 derived from various animal species in LLC-PK1. *Pharmaceutical research* **23:**1460-1472.

Tiden AK, Sjogren T, Svensson M, Bernlind A, Senthilmohan R, Auchere F, Norman H, Markgren PO, Gustavsson S, Schmidt S, Lundquist S, Forbes LV, Magon NJ, Paton LN, Jameson GN, Eriksson H, and Kettle AJ (2011) 2-thioxanthines are mechanism-based inactivators of myeloperoxidase that block oxidative stress during inflammation. *The Journal of biological chemistry* **286:**37578-37589.

Varma MV, Feng B, Obach RS, Troutman MD, Chupka J, Miller HR, and El-Kattan A (2009) Physicochemical determinants of human renal clearance. *Journal of medicinal chemistry* **52:**4844-4852.

Varma MV, Gardner I, Steyn SJ, Nkansah P, Rotter CJ, Whitney-Pickett C, Zhang H, Di L, Cram M, Fenner KS, and El-Kattan AF (2012) pH-Dependent solubility and permeability criteria for provisional biopharmaceutics classification (BCS and BDDCS) in early drug discovery. *Molecular pharmaceutics* **9:**1199-1212.

Varma MV, Rotter CJ, Chupka J, Whalen KM, Duignan DB, Feng B, Litchfield J, Goosen TC, and El-Kattan AF (2011) pH-sensitive interaction of HMG-CoA reductase inhibitors (statins) with organic anion transporting polypeptide 2B1. *Molecular pharmaceutics* **8:**1303-1313.

Varma MV, Steyn SJ, Allerton C, and El-Kattan AF (2015) Predicting Clearance Mechanism in Drug Discovery: Extended Clearance Classification System (ECCS). *Pharmaceutical research*.

Waldhauser L and Uetrecht J (1991) Oxidation of propylthiouracil to reactive metabolites by activated neutrophils. Implications for agranulocytosis. *Drug metabolism and disposition: the biological fate of chemicals* **19:**354-359.

Walsky RL and Obach RS (2004) Validated assays for human cytochrome P450 activities. *Drug metabolism and disposition: the biological fate of chemicals* **32:**647-660.

Wolf RL, King BF, Torres VE, Wilson DM, and Ehman RL (1993) Measurement of normal renal artery blood flow: cine phase-contrast MR imaging vs clearance of p-aminohippurate. *AJR American journal of roentgenology* **161:**995-1002.

Footnotes

§At the time of data generation, all authors were employees and stockholders of Pfizer Inc. Pfizer Inc. provided support in the form of salaries for the authors but did not have any additional role in the study design, data collection and analysis, decision to publish, or preparation of the manuscript.

This study was sponsored by Pfizer.

DMD Fast Forward. Published on November 25, 2015 as DOI: 10.1124/dmd.115.067868
This article has not been copyedited and formatted. The final version may differ from this version.

Figure Legends

Fig. 1. Structure of PF-06282999 and mechanism of MPO inactivation by 2-thioxanthines.

Fig. 2. Mean (± SD) plasma PF-06282999 concentration-time profiles after single dose oral administration of solution formulation of PF-06282999 at 20, 50, 125, and 200 mg to human subjects (n = 6) in linear (panel A) and log-linear scale (panel B).

Fig. 3. Panel A. Dose-proportionality of pharmacokinetic parameters AUC and C_{max} observed after single dose oral administration of 20 to 200 mg PF-06282999 to human subjects (n = 6). Data are presented as mean ± SD. Panel B. Urinary excretion of PF-06282999 as unchanged drug (% of dose) after single dose oral administration of 20 to 200 mg PF-06282999 to human subjects (n = 6). Data are presented as mean ± SD.

DMD Fast Forward. Published on November 25, 2015 as DOI: 10.1124/dmd.115.067868
This article has not been copyedited and formatted. The final version may differ from this version.

TABLES

TABLE 1

Clinical study treatment assignment for PF-06282999

Cohort	Sequence	*n*	Period 1	Period 2	Period 3	Period 4
1	1	2	Placebo	50 mg	125 mg	200 mg
	2	2	20 mg	Placebo	125 mg	200 mg
	3	2	20 mg	50 mg	Placebo	200 mg
	4	2	20 mg	50 mg	125 mg	Placebo

n = number of subjects.

TABLE 2

Mass spectral characteristics of the in vitro metabolites of PF-06282999

Metabolite	MH+	Retention time (t_R), min	Structure	Fragment Ions
Parent	326.0361	29.0	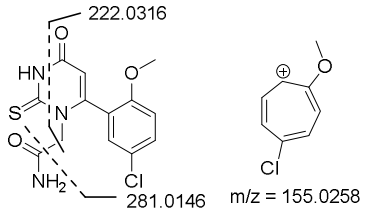	281.0144, 222.0315, 155.0256
M1	296.0433	21.9	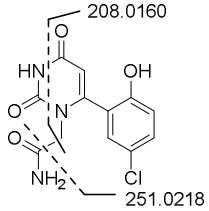	251.0214, 235.0265 (-S), 208.0156
M2	312.0204	24.1	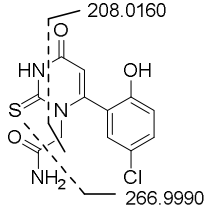	266.9986, 208.0157

M3[a]	310.0589	25.7	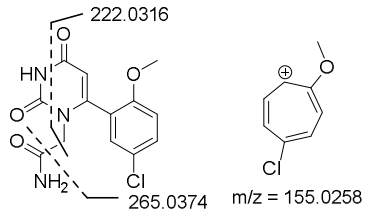	265.0372, 222.0314, 155.0253

All metabolites were observed in liver microsomes and hepatocytes from preclinical species and human. [a]The structure of M3 was unambiguously confirmed by comparison of its LC-MS/MS characteristics with an authentic standard.

DMD Fast Forward. Published on November 25, 2015 as DOI: 10.1124/dmd.115.067868
This article has not been copyedited and formatted. The final version may differ from this version.

TABLE 3

Permeability and transporter data of PF-06282999 in Caco-2, MDCKII-LE and MDCKII-MDR1 cell monolayer

Compound	A-to-B P_{app} ($x10^{-6}$ cm/s)	B-to-A P_{app} ($x10^{-6}$ cm/s)	Efflux Ratio	Fold Change from A-to-B at pH 7.4)
Caco-2				
PF-06282999 (pH 7.4)	2.7	10	3.8	
PF-06282999 (pH 6.0)	2.7			1.0
PF-06282999 (pH 7.4, Ca^{2+}-free)	12			4.4
PF-06282999 (pH 7.4) + MDR1 Inhibitors	2.9	7.6	2.6	1.1
MDCKII-LE				
PF-06282999 (pH 7.4)	2.2			
MDCKII-MDR1				
PF-06282999 (pH 7.4)	0.6	2.1	3.3	

DMD Fast Forward. Published on November 25, 2015 as DOI: 10.1124/dmd.115.067868
This article has not been copyedited and formatted. The final version may differ from this version.

TABLE 4

Hepatobiliary disposition of PF-06282999 in SCHH

Compound	Apparent intrinsic uptake clearance (µl/min/mg protein)	Passive uptake clearance (µl/min/mg protein)[a]	Active uptake (%)	Apparent intrinsic biliary clearance (µl/min/mg protein)	BEI (%)
PF-06282999	2.3	1.7	25	0.2	11
Rosuvastatin	8.5	0.9	89	3.5	49

[a]Uptake was measured in the presence of rifamycin SV (100 µM).

TABLE 5

Preclinical pharmacokinetics of PF-06282999

Species[a]	C_{max} (ng/ml)[b]	T_{max} (h)[b]	Oral $AUC_{0-\infty}$ (ng·h/ml)[b]	CL_p (ml/min/kg)	Vd_{ss} (l/kg)	$t_{1/2}$ (h)	Oral F (%)[b]
Mouse	3650 ± 325	1.0 ± 0.1	24800 ± 1010	10.1 ± 0.83	0.90 ± 0.06	1.36 ± 0.12	>100
Rat	596 ± 282	1.1 ± 0.88	1780 ± 287	41.8 ± 9.65	2.13 ± 1.08	0.75 ± 0.19	86
Dog	4090 ± 979	0.7 ± 0.3	11800 ± 3480	3.39 ± 1.13	0.54 ± 0.04	2.2 ± 0.5	75
Monkey	771 (1040, 501)	1.5 (1.0, 2.0)	3720 (4130,3300)	10.3 (10.5,10.1)	1.09 (1.17, 1.01)	3.32 (5.22, 1.42)	76

[a]All experiments involving animals were conducted in our AAALAC-accredited facilities and were reviewed and approved by Pfizer Institutional Animal Care and Use Committee. Pharmacokinetic parameters were calculated from plasma concentration–time data and are reported as mean (± S.D. for *n*=3 and maximum values for *n*=2). All pharmacokinetics were conducted in male gender of each species (Wistar rats, CD-1 mice, Beagle dogs, and/or cynomolgus monkey). Intravenous (i.v.) doses for PF-06282999 were 1 mg/kg and were administered as a solution. Oral (p.o.) doses for PF-06282999 were 3 or 5 mg/kg and were formulated in 5% HPMC in 20 mM Tris/0.5% HPMCAS. [b]Obtained from p.o. dose.

DMD Fast Forward. Published on November 25, 2015 as DOI: 10.1124/dmd.115.067868
This article has not been copyedited and formatted. The final version may differ from this version.

TABLE 6

Renal excretion of unchanged PF-06282999 in preclinical species after i.v. administration

Species	Renal excretion (% of total dose)	Total CL_p (ml/min/kg)	Total CL_{renal} (ml/min/kg)[a]	Unbound CL_{renal} (ml/min/kg)[b]	Unbound CL_{renal}/GFR ratio[c]
Mouse	44.2	10.1	4.03	9.8	1.0
Rat	30.5	41.8	11.6	28	3.2
Dog	26.0	3.39	0.96	1.9	0.5
Monkey	19.5	10.3	1.67	3.7	1.86

[a]Total CL_{renal} in blood was estimated by multiplying the total CL_b with fraction of total i.v. dose of unchanged PF-06282999 excreted in urine. CL_b was obtained by dividing CL_p by the blood to plasma ratio in the individual animal species (mouse B:P = 1.1, rat B:P = 1.1, dog B:P = 0.91, monkey B:P = 1.2).

[b]Unbound CL_{renal} in blood was estimated by normalizing total CL_{renal} with the unbound free fraction in blood (mouse = 0.41, rat = 0.41, dog = 0.51, monkey = 0.45), which in turn was obtained by dividing the unbound plasma free fraction by the blood to plasma ratio.

[c]GFR values (ml/min/kg) in rats, mice, dogs, and monkeys are 8.7, 10, 4.0, and 2.0.

DMD Fast Forward. Published on November 25, 2015 as DOI: 10.1124/dmd.115.067868
This article has not been copyedited and formatted. The final version may differ from this version.

TABLE 7

Prediction of human pharmacokinetics and CLrenal for PF-06282999

Predicted Human Pharmacokinetics Parameter[a]	Rat	Dog	Monkey
CL_p (ml/min/kg)	8.6	1.8	3.4
Vd_{ss} (l/kg)	1.8	0.4	0.8
$t_{1/2}$ (h)	2.4	2.6	2.7
total CL_{renal} (ml/min/kg)[b]	3.0	0.6	0.7

[a]Observed pharmacokinetics in human: CL_p = 1.8–2.1 ml/min/kg, Vd_{ss} = 0.65–0.78 l/kg (20–200 mg p.o. doses) obtained from the respective CL/F and Vz/F values normalized for F values corresponding to the percentage of dose eliminated in unchanged form in urine in a 24 h period at the respective p.o. doses. Human $t_{1/2}$ was estimated to be 3.9–4.2 h (20–200 mg p.o. doses) and calculated using the equation 0.693 x Vd_{ss}/CL_p.

[b]Observed total CL_{renal} in human = 1.8–2.1 ml/min/kg (20–200 mg p.o. doses).

DMD Fast Forward. Published on November 25, 2015 as DOI: 10.1124/dmd.115.067868
This article has not been copyedited and formatted. The final version may differ from this version.

TABLE 8

Summary of plasma pharmacokinetics of PF-06282999 in healthy fasted male subjects after single p.o. doses administered as solution

Dose	$AUC_{0-\infty}$ (ng·h/ml)[a]	C_{max} (ng/ml)[a]	T_{max} (h)[b]	$t_{1/2}$ (h)[c]	CL/F (ml/min)[a]	V_z/F (l)[a]
20 mg	1792 (363)	402 (131)	0.75 (0.5, 1.1)	4.3 (0.7)	186 (44)	68.9 (10.8)
50 mg	4294 (664)	920 (232)	0.5 (0.5, 1.0)	4.4 (0.6)	194 (34)	73.6 (11.5)
125 mg	10730 (1950)	2659 (631)	0.5 (0.5, 1.0)	4.4 (0.6)	194 (40)	73.7 (7.5)
200 mg	16950 (2880)	3799 (1156)	0.5 (0.5, 2.0)	4.3 (0.4)	197 (32)	72.6 (7.2)

[a]Geometric mean (S.D.) for AUC, C_{max}, CL/F and V_z/F.

[b]Median (range) for T_{max}.

[c]Arithmetic mean (S.D.) for $t_{1/2}$.

DMD Fast Forward. Published on November 25, 2015 as DOI: 10.1124/dmd.115.067868
This article has not been copyedited and formatted. The final version may differ from this version.

TABLE 9

Summary of urinary excretion of PF-06282999 in healthy fasted male subjects after single p.o. doses administered as solution

Dose	$A_{e,\ urine,\ (0\text{-}24h)}$ (mg)[a]	$A_{e,\ urine,\ (0\text{-}24h)}$ (% of dose)[a]	CL_{renal} (ml/min)[a]	$CL_{renal,u}$ (ml/min)[b]
20 mg	13.3 (1.7)	66.7 (8.5)	127 (18)	338
50 mg	36.3 (3.2)	72.4 (6.4)	144 (14)	383
125 mg	86.9 (8.3)	69.5 (6.6)	138 (26)	367
200 mg	151.1 (12.6)	75.5 (6.2)	151 (21)	402

[a]Geometric mean (S.D.) for all parameters. [b]$CL_{renal,u}$ estimated by dividing CL_{renal} by human plasma unbound fraction of 0.376.

Figure 1

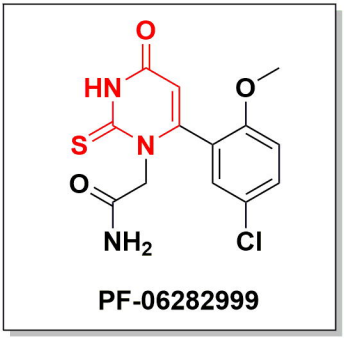

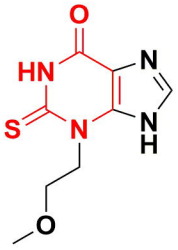

TX5

MPO

H_2O_2 H_2O

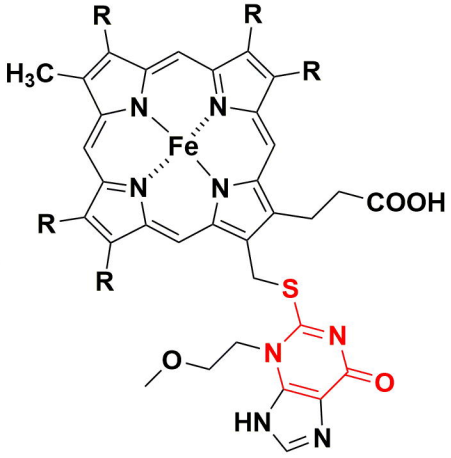

MPO Heme Adduct

(Inactive Enzyme)

Figure 2

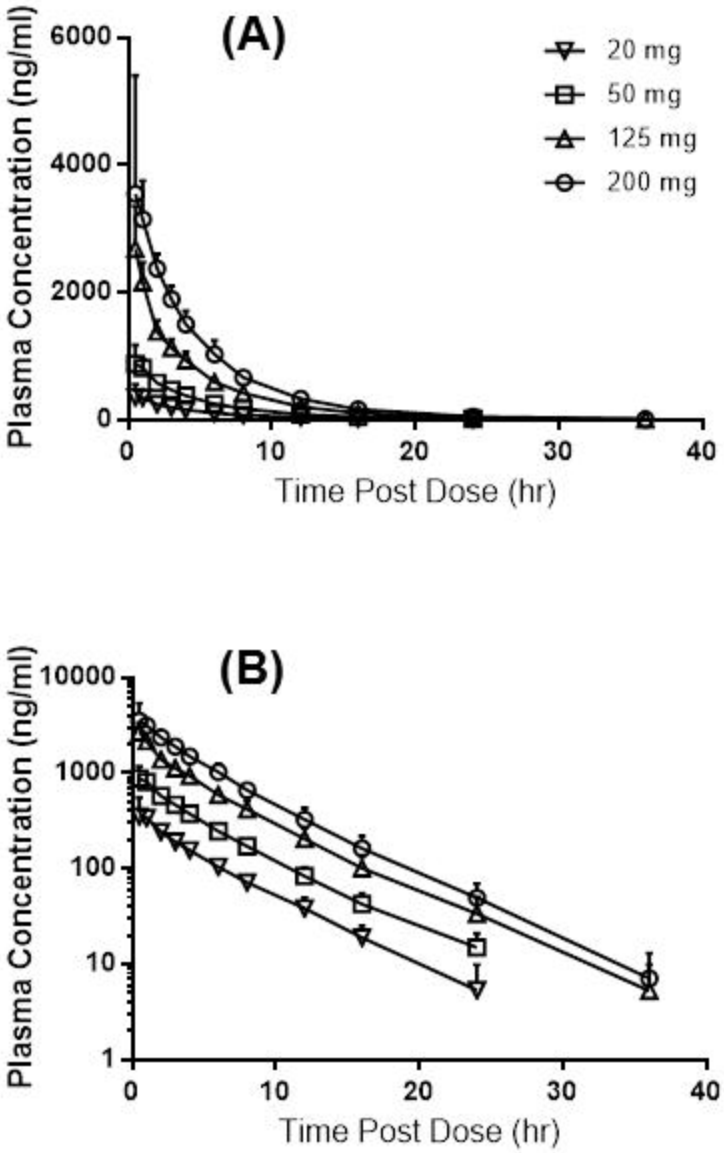

Figure 3